EUROPEAN ORGANIZATION FOR NUCLEAR RESEARCH

L3 Note 2421
June 15, 1999

Measurement of Charm and Beauty Production in $\gamma\gamma$ Collisions at LEP

The L3 Collaboration

Abstract

Inclusive heavy flavour production in $\gamma\gamma$ collisions has been studied with the L3 detector at the LEP collider. Preliminary results on charm and beauty production at $\sqrt{s} = 189$ GeV are presented. Hadronic final states containing charm and beauty particles were identified by detecting electrons or muons from their semi-leptonic decays. Charm particles in the final state were also identified by the reconstruction of charged D^* meson decays. The cross section of charm production with a D^* tag is in agreement with the lepton tag measurement. The cross section of beauty production in $\gamma\gamma$ collisions has been measured for the first time. Even including real and virtual gluon emission (NLO QCD) the direct process $\gamma\gamma \rightarrow c\bar{c}, b\bar{b}$ is insufficient to describe charm and beauty production in $\gamma\gamma$ collisions. The measured cross section and event distributions require resolved processes, sensitive to the gluon density function of the photon.

Submitted to *International Europhysics Conference High Energy Physics 99*
Tampere, Finland, 15-21 July 1999.

1 Introduction

The production of heavy quarks in two-photon collisions consists mainly of charm quarks. Because of their smaller electric charge and larger mass, the production of b-quarks is expected to be suppressed by more than two orders of magnitude relative to the production of charm quarks [1]. The measurement of heavy flavour production in two-photon collisions provides a good test of QCD because the large physical scale set by the charm (beauty) quark mass makes the perturbative calculations reliable. At LEP energies, the direct and resolved processes (Figure 1) are predicted to give comparable contributions to the cross section [1]. The contributions to heavy flavour production from soft processes described by the Vector Dominance Model (VDM) and from doubly resolved processes are expected to be small. The resolved photon cross section is dominated by the photon-gluon fusion diagram $\gamma \mathrm{g} \to \mathrm{c\bar{c}}, \mathrm{b\bar{b}}$. The production rate of charm (beauty) quarks in two-photon collisions depends on the charm (beauty) quark mass and on the gluon density in the photon. Measurements of charm production in two-photon collisions were done at PEP, PETRA, TRISTAN and LEP [2–9], where charm quarks were identified by charged D^* mesons, inclusive electrons or muons and $\mathrm{K^0_S}$ mesons. Beauty production in $\gamma\gamma$ collisions has been never measured before.

In this paper we present the preliminary result of the measurement of the $\mathrm{e^+e^- \to e^+e^-c\bar{c}}$ and $\mathrm{e^+e^- \to e^+e^-b\bar{b}}$ cross section by the L3 experiment at $\sqrt{\mathrm{s}} = 189$ GeV. We identify charm and beauty quarks by tagging electrons [1)] and muons from semileptonic charm and beauty decays. Charm particles in the final state were also identified by the reconstruction of charged D^* meson decays. The data correspond to a total integrated luminosity of $\mathcal{L} = 176\ \mathrm{pb}^{-1}$.

2 Charm and Beauty Production by Lepton tag

2.1 Selection of Hadronic Two-Photon Events

The L3 detector has been described in detail in Ref. [10]. The L3 measurement of charm production at 91 GeV $\leq \sqrt{s} \leq$ 183 GeV has been published in [9]. The event selection is done in two steps. The first one selects hadronic final states produced in two-photon collisions, and the second identifies a charm or a beauty quark. Hadronic two-photon events are selected by cuts on the number of tracks, the visible energy and the visible mass. The visible energy, $\mathrm{E_{vis}}$, is the sum of the energies measured in the calorimeters and that of the muons measured in the muon spectrometer. The visible mass, $\mathrm{W_{vis}}$, of the event is calculated from the four-momentum vectors of the measured calorimetric clusters. All particles are considered to be pions except for electromagnetic (EM) clusters identified as photons. We require at least five tracks in each event; the visible energy has to be less than $0.38\sqrt{s}$ and the visible mass has to be greater than 3 GeV. The cut on $\mathrm{E_{vis}}$ separates the two-photon from annihilation processes which are characterized by high visible energy. The data are reasonably well described by the simulation of the $\gamma\gamma \to$ hadrons contribution and annihilation processes background. The background from $\mathrm{e^+e^- \to e^+e^-}\tau^+\tau^-$ and $\mathrm{e^+e^-} \to \tau^+\tau^-$ events is highly suppressed by the five tracks requirement.

The analysis is limited to untagged events with small photon virtuality. Events are excluded when the most energetic cluster in the L3 luminosity monitor has an energy greater than 0.4 $\mathrm{E_{beam}}$. Thus the interacting photons are quasi-real: $\langle \mathrm{Q}^2 \rangle \cong 1.510^{-2}\ \mathrm{GeV}^2$, where $-\mathrm{Q}^2$ is the invariant mass squared of the virtual photon.

[1)] Electron stands for electron or positron throughout this paper.

Background sources are the two-photon process $e^+e^- \rightarrow e^+e^-\tau^+\tau^-$ simulated with the JAMVG [11] Monte Carlo generator, and the annihilation processes $e^+e^- \rightarrow Z/\gamma \rightarrow q\bar{q}$, simulated with PYTHIA 5.7 [12]. The process $e^+e^- \rightarrow \tau^+\tau^-$ is simulated with KORALZ [13], and $e^+e^- \rightarrow W^+W^-$ with KORALW [14]. After the hadron selection, the background from the annihilation processes and the two-photon production of tau pairs is below 1%.

The PYTHIA Monte Carlo simulates two-photon events according to the current knowledge of hadronic interactions obtained by pp and γp studies [12]. The two-photon processes are generated with massless ($m_q = 0$) matrix elements [15]. The resolved process uses the SaS1d photon structure function [16]. We have implemented the two-photon luminosity function in the equivalent photon approximation (EPA) which has a cutoff: $Q^2 < m_\rho^2$ [17].

The detector simulation was performed by a GEANT-based description of the L3 detector [18]. The Monte Carlo events are reconstructed in the same way as the data.

2.2 Electron Selection

To identify charm-quark production, we search for an electron with momentum greater than 0.6 GeV in the polar angle range $|\cos\theta| < 0.9$. Electron candidates are selected as follows:

- The EM cluster is required to match with a track; the difference between the azimuthal angles estimated from the shower barycentre and from the track impact point at the calorimeter must be smaller than 20 mrad.

- To confirm that a shower in the EM calorimeter is created by an electron, the distribution of energies measured in the crystals of the calorimeter are compared to that of an EM cluster using a χ^2 test.

- The cluster must also satisfy the condition $0.85 < E_t/p_t < 1.20$ (Figure 2), where E_t is the projection of the energy of the cluster on the r-ϕ plane and p_t is the transverse momentum of the track as measured in the central tracker. This condition rejects more than 95% of the hadrons (mainly pions) while keeping more than 90% of the electrons. The average resolutions for the selected electron candidates are 4.6% on p_t and 3.3% on E_t.

- The distance of closest approach of the track to the average position of the e^+e^- collision point in the r-ϕ plane must be less than 0.5 mm. This cut rejects 71% of electron candidates from γ conversions while keeping more than 88% of signal electrons.

After all cuts are applied 1710 events remain. The trigger efficiency is $87 \pm 3\%$. The background from the annihilation processes and the two-photon production of tau pairs is about 1%. We assume that this background has the same trigger efficiency as hadronic two-photon signal events. The electron purity is 85%. The absolute prediction for the number of events is smaller by a factor 1.6; this difference can be attributed to the fact that the PYTHIA Monte Carlo contains only leading order calculations.

2.3 Muon Selection

Only muons with momentum greater than about 2 GeV can penetrate the calorimeters and reach the muon chambers. In order to suppress the contribution from the annihilation processes, we require the muon momentum to be less than 0.2 E_{beam}. The angular acceptance is limited to $|\cos\theta| < 0.9$.

After all cuts are applied 208 events remain. The polar angle distribution of selected muons is given in Figure 3. The trigger efficiency is higher by a factor 1.08 than in the case of the electron selection due to the higher momentum cut. The muon purity is 96%. The background from annihilation processes and two-photon production of tau pairs is 9%.

2.4 The charm cross section measurement

The total cross section of inclusive charm production is calculated from the following equation:

$$\sigma = \frac{(N_{\mathrm{obs}}^{\mathrm{lept}} - N_{\mathrm{bkg}}^{\mathrm{lept}})\ \pi_{\mathrm{c}}}{\mathcal{L}\ \epsilon_{\mathrm{trig}}\ \epsilon'_{\mathrm{c}}}. \tag{1}$$

The variables are defined as follows:

- $N_{\mathrm{obs}}^{\mathrm{lept}}$ is the number of events in the data after the final lepton selection.
- ϵ_{trig} is the trigger efficiency which is determined from the data using a set of independent triggers.
- $N_{\mathrm{bkg}}^{\mathrm{lept}}$ is the number of background events estimated from Monte Carlo which do not originate from two-photon hadronic interactions.
- $\mathcal{L}$ is the total integrated luminosity.

The charm selection efficiency, ϵ'_{c}, is the fraction of charm events selected by the lepton tag analysis relative to the events generated in the full phase space. The charm purity, π_{c}, is defined as:

$$\pi_{\mathrm{c}} = \frac{N_{\mathrm{c}}^{\mathrm{lept}}}{N_{\mathrm{c}}^{\mathrm{lept}} + N_{\mathrm{nc}}^{\mathrm{lept}}}. \tag{2}$$

In order to be less dependent on the Monte Carlo flavour composition (charm to non-charm fraction), the charm purity can be rewritten as:

$$\pi_{\mathrm{c}} = (1 - \frac{\epsilon_{\mathrm{nc}}}{\epsilon_{\mathrm{d}}})/(1 - \frac{\epsilon_{\mathrm{nc}}}{\epsilon_{\mathrm{c}}}), \tag{3}$$

where the ϵ_{c} (ϵ_{nc}) is the fraction of charm $N_{\mathrm{c}}^{\mathrm{lept}}$ (non-charm $N_{\mathrm{nc}}^{\mathrm{lept}}$) events, accepted by the final selection from the charm (non-charm) events obtained after the hadronic selection. The quantity ϵ_{d} is defined by the relation:

$$\epsilon_{\mathrm{d}} = \frac{N_{\mathrm{c}}^{\mathrm{lept}} + N_{\mathrm{nc}}^{\mathrm{lept}}}{N_{\mathrm{c}}^{\mathrm{had}} + N_{\mathrm{nc}}^{\mathrm{had}}} = \frac{N_{\mathrm{obs}}^{\mathrm{lept}} - N_{\mathrm{bkg}}^{\mathrm{lept}}}{N_{\mathrm{obs}}^{\mathrm{had}} - N_{\mathrm{bkg}}^{\mathrm{had}}} \tag{4}$$

and can thus be determined directly from the data. The equation (4) is obtained by noticing that the total number of selected hadronic events $N_{\mathrm{c}}^{\mathrm{had}} + N_{\mathrm{nc}}^{\mathrm{had}}$ can be expressed as:

$$\frac{N_{\mathrm{c}}^{\mathrm{lept}} + N_{\mathrm{nc}}^{\mathrm{lept}}}{\epsilon_{\mathrm{d}}} = \frac{N_{\mathrm{c}}^{\mathrm{lept}}}{\epsilon_{\mathrm{c}}} + \frac{N_{\mathrm{nc}}^{\mathrm{lept}}}{\epsilon_{\mathrm{nc}}}. \tag{5}$$

This method of deriving the charm cross section is insensitive to the absolute normalization of the charm and background Monte Carlo, but still depends on the ratio of direct to resolved processes in the signal Monte Carlo, as discussed below.

The charm purity is 0.67 for electrons and 0.64 for muons [2)]. The purity calculated with the use of ϵ_{d} from the data gives on average a value about 10% higher than the estimate using only the Monte Carlo. For the electron sample, the charm selection efficiency ϵ'_{c} is 0.5%, this efficiency is much lower for the muon sample, about 0.07%, due to the higher momentum cut.

The resulting cross sections are

$$\sigma^{ee\to eeccX}_{electron-tag} = 1599 \pm 60 \text{ (stat) } \pm 174 \text{ (syst) pb}$$

$$\sigma^{ee\to eeccX}_{muon-tag} = 1070 \pm 144 \text{ (stat) } \pm 152 \text{ (syst) pb}$$

The combined value for the lepton tag is

$$\sigma^{ee\to eeccX} = 1378 \pm 55 \text{ (stat) } \pm 134 \text{ (syst) pb}$$

Systematic errors arise from the uncertainty on background subtraction, selection efficiencies, trigger efficiency, cut variation and charm semileptonic branching ratio. The average charm semileptonic branching ratio used in the simulation is 0.098 [19]. The dominant systematic errors for the electron sample are from the cut variation and selection efficiencies. The dominant systematic error for the muon sample comes from selection efficiencies.

The charm production cross sections are obtained with the PYTHIA Monte Carlo using a massless quark matrix element calculation. The effect of the use of massive matrix elements is tested by using the PYTHIA Monte Carlo events generated with the charm mass $\mathrm{m_c} = 1.6$ GeV. Since the cross section values are dependent on the ratio of the charm purity to the charm selection efficiency, $\pi_{\mathrm{c}}/\epsilon'_{\mathrm{c}}$, we compare the value of this ratio using the massless matrix elements to the ratios obtained from the massive matrix elements approach. Within statistics they are the same. A change of the direct to resolved process ratio in the signal Monte Carlo by a factor 1.2 (1.4) results in a change of the charm cross section by 3.4% (6%) for electrons and has negligible effect for muons.

The PYTHIA Monte Carlo is the only generator available which includes all hadronic two-photon processes relevant in this analysis. The QED JAMVG program generates only the direct process. To better understand possible systematics due to the different models, we have compared the values of $\pi_{\mathrm{c}}/\epsilon'_{\mathrm{c}}$ for the direct process as given by PYTHIA and by JAMVG. There is agreement within 10% which is comparable with the statistical uncertainty. However, for low momenta as seen in the case of the electron selection, the value of $\pi_{\mathrm{c}}/\epsilon'_{\mathrm{c}}$ for the direct process is two times higher than that for the resolved process.

The most sensitive distributions where predictions for direct and resolved processes are different are found to be the visible mass, the track multiplicity, the transverse momentum of the lepton and the energy flow spectra. These distributions agree well with PYTHIA and are incompatible with direct process only [9].

The total inclusive charm production cross sections are plotted in Figure 9 together with previous measurements [2–9]. For the purpose of comparison, the published results of different experiments were extrapolated to the total charm cross sections using the procedure of Ref. [20]. The data are compared to the predictions of Ref. [1]. The dashed line corresponds to the direct process, NLO QCD calculations, while the solid line shows the QCD prediction for the sum of direct and resolved processes calculated to NLO accuracy. The direct process depends upon the heavy-quark mass and the QCD coupling constant. The prediction is calculated using a charm

[2)] Besides charm quark semileptonic decays other sources of electrons and muons are the decays $\tau^+ \to l^+\nu_l\bar{\nu}_\tau, \pi^+ \to \mu^+\nu_\mu, \pi^0 \to e^+e^-\gamma, K^+ \to \mu^+\nu_\mu, l^+\pi^0\nu_l, K^0_L \to l^+\pi^-\nu_l, ...$

mass of 1.3 GeV; the open charm threshold energy is set to 3.8 GeV. For a charm mass of 1.7 GeV the cross section is 35 % lower at $\sqrt{s} = 189$ GeV. The theory prediction for the resolved process was calculated with the parton density function of Glück-Reya-Vogt [21]. Using the Drees-Grassie [22] parametrization for the photon parton density results in a decrease of the cross section of 9% for $\mathrm{m_c} = 1.3$ GeV and of 3% for $\mathrm{m_c} = 1.7$ GeV. The renormalization scale was chosen to be the charm mass. A change in the renormalization scale from $\mathrm{m_c}$ to $2\mathrm{m_c}$ decreases the QCD prediction by 30% (15%) for $\mathrm{m_c} = 1.3$ (1.7) GeV. The uncertainties in the calculations indicate that it is not possible to determine the mass of the charm quark simply by measuring the total charm cross section.

2.5 The beauty production measurement

Leptons from b semi-leptonic decays are more energetic than from charm semi-leptonic decays and non-charm two-photon processes. Figure 4 shows the electron and muon momentum distributions from semi-leptonic decays in $b\bar{b}$ and $c\bar{c}$ events (JAMVG Monte Carlo [11] generator). The transverse momentum of the lepton relative to the b jet is also bigger due to the higher b quark mass and harder b fragmentation function.

To select $b\bar{b}$ events we apply cuts on the lepton momentum and transverse momentum p_t with respect to the closest jet defined by excluding the lepton from the jet. The jets are reconstructed by the JADE algorithm with cut $y = 0.1$. Figure 5 shows an electron and muon transverse momentum with respect to the closest jet. The solid histogram is the contribution from all flavours including b, while the dashed histogram is the PYTHIA prediction for uds quarks plus charm. The charm fraction in the PYTHIA Monte Carlo has been scaled to the measured charm cross section (see section 2.3). The cuts are defined by minimizing the statistical error on the cross section measurement. The lepton momentum must be greater than 2 GeV for electrons and 2.5 GeV for muons, the transverse momentum p_t greater than 1 GeV and 1.5 GeV for electrons and muons, respectively.

The observed number of events is 96 for the electron tag and 49 for the muon tag. The beauty purities (selection efficiencies) are 28 % (1.6 %) and 34 % (0.9 %) for electron and muon samples, respectively. One can see from the Figure 5 that the beauty purity increases with the transverse momentum. The beauty cross section has been calculated following equation 1. The preliminary beauty production cross section in $\gamma\gamma$ collisions has been measured to be

$$\sigma^{ee \to eebbX}_{electron-tag} = 9.6 \pm 3.6 \text{ (stat) } \pm 4.1 \text{ (syst) pb}$$

$$\sigma^{ee \to eebbX}_{muon-tag} = 10.3 \pm 4.6 \text{ (stat) } \pm 3.3 \text{ (syst) pb}$$

The combined value is

$$\sigma^{ee \to eebbX} = 9.9 \pm 2.9 \text{ (stat) } \pm 3.8 \text{ (syst) pb}$$

Systematic errors arise from the uncertainty on selection efficiencies, trigger efficiency, cut variation and ratio of the direct to resolved fraction. The results plotted in Figure 9 lie somewhat above QCD predictions.

3 Charm production by D^* tag

As in the case of the lepton tag the D^* event selection proceeds in two steps. First to select hadronic two-photon events the energy deposited in the hadronic calorimeter must be less than

40 GeV and the energy deposited in the electromagnetic calorimeter 0.5 GeV $\leq E_{ECAL} \leq$ 30 GeV. The transverse visible energy imbalance has to be smaller than 12.5 GeV. The visible mass has to be greater than 2 GeV and at least three tracks must be reconstructed in the L3 central tracker. In order to reduce combinatorial background we require an event track multiplicity to be less than 16.

The $D^{*\pm}$ is then reconstructed in the decay channel $D^{*+} \rightarrow D^0\pi^+ \rightarrow K^-\pi^+\pi^+$ with a mass difference technique [23]. To select D^0 candidates two oppositely charged tracks, identified as kaon and pion by dE/dx, must have an invariant mass $m_{D^0} \pm 50$ MeV. The decay vertex of the D^0 candidate has to be close to the primary vertex. We require the D^0 candidate impact parameter to be less than 0.6 mm in the transverse plane. A signed distance l between D^0 decay vertex and the D^0 point of the closest approach to the primary vertex has to satisfy the condition -0.9 mm $\leq l \leq$ 1.1 mm. The primary vertex is defined as the average beam position in the LEP fill.

After the D^0 candidate is selected the slow pion from the $D^{*\pm}$ decay is identified as a pion by dE/dx. A slow pion candidate is selected with momentum greater than 70 MeV, distance of closest approach to the primary vertex in the transverse plane less than 3 mm, and a charge opposite to the kaon charge. The momentum of the $D^{*\pm}$ candidate must be greater than 1.3 GeV.

Figure 6 shows the mass difference between the D^* and the D^0 candidates in the data. The D^* signal is well identified as the peak at about 145 MeV. The shape of the background is determined from the D^0 sideband and from the D^0 wrong charge combinations (same sign kaon-pion pair). It is shown by the shaded histogram. The fit gives a signal of 68 ± 10 $D^{*\pm}$ candidates. The same procedure has been applied to the Monte Carlo in order to determine the D^* selection efficiency.

The cross section of charm production with D^* tag is calculated using the equation:

$$\sigma = \frac{N_{\rm obs}^{D^{*\pm}}}{\mathcal{L}\ \epsilon_{\rm trig}\ \epsilon_{D^{*\pm}}\ 2\ P(c \rightarrow D^{*+})}, \qquad (6)$$

where $\mathcal{L}$ is the integrated data luminosity, $\epsilon_{\rm trig}$ is the trigger efficiency, $P(c \rightarrow D^{*+})$ is the probability of the charm quark to fragment into D^* and $N_{\rm obs}^{D^{*\pm}}$ is the number of $D^{*\pm}$ candidates from the fit. The efficiency $\epsilon_{D^{*\pm}}$, determined with the PYTHIA Monte Carlo, is $\epsilon_{D^{*\pm}} = (7.2 \pm 0.9)10^{-4}$. The charm production cross section is measured to be

$$\sigma_{D^*-tag}^{ee\rightarrow eeccX} = 1269 \pm 185\ (\text{stat})\ \pm 343\ (\text{syst})\ \text{pb}$$

The systematic error arise from selection efficiency (12.5 %), background subtraction (17.6 %), resolved process fraction (15.5 %), trigger efficiency (3.4%) and probability $P(c \rightarrow D^{*+}) = 0.243 \pm 0.009$ [24]. The cross section agrees well with the measurement by lepton tag and with QCD expectation (Figure 9).

In Figure 7 the D^* candidate transverse momentum and the event visible mass distributions are compared with PYTHIA prediction for the direct process only and for all processes included. In both cases the Monte Carlo is normalized to the number of data events. Figure 8 shows the data versus Monte Carlo comparison for the ratio $p_t^{D^*}/W_{vis}$. In both figures it is evident that the direct process alone can not describe the data, while the full PYTHIA model reproduces the data correctly.

4 Conclusions

The cross section for inclusive charm and beauty production in two-photon collisions, $\sigma(\mathrm{e^+e^-} \rightarrow \mathrm{e^+e^-c\bar{c}})$ and $\sigma(\mathrm{e^+e^-} \rightarrow \mathrm{e^+e^-b\bar{b}})$, is measured with the L3 detector at $\sqrt{s} = 189$ GeV. The charm production is identified by a lepton tag (electron and muon), and by the D^* signal. The b is identified by high momentum and high transverse momentum leptons. The results are preliminary.

The direct process $\gamma\gamma \rightarrow \mathrm{c\bar{c}}, \mathrm{b\bar{b}}$ is insufficient to describe the data, even if real and virtual gluon corrections are included. The cross sections and the event distributions require contributions from the resolved processes which are dominantly $\gamma\mathrm{g} \rightarrow \mathrm{c\bar{c}}, \mathrm{b\bar{b}}$. The data therefore require a significant gluon content in the photon.

The $b\bar{b}$ cross section is measured here for the first time in two-photon collisions. The measured b cross section lie somewhat above QCD predictions.

Acknowledgments

We wish to express our gratitude to the CERN accelerator divisions for the excellent performance of the LEP machine. We also acknowledge and appreciate the effort of all the engineers, technicians and support staff who have participated in the construction and maintenance of this experiment.

References

[1] M. Drees, M. Krämer, J. Zunft and P.M. Zerwas, Phys. Lett. B **306**, (1993) 371.

[2] JADE Collab., W. Bartel et al., Phys. Lett. B **184**, (1987) 288.

[3] TPC/Two-Gamma Collab., M. Alston-Garnjost et al., Phys. Lett. B **252**, (1990) 499.

[4] TASSO Collab., W. Braunschweig et al., Z. Phys. C **47**, (1990) 499.

[5] TOPAZ Collab., R. Enomoto et al., Phys. Lett. B **328**, (1994) 535, Phys. Rev. D **50**, (1994) 1879, Phys. Lett. B **341**, (1994) 99, Phys. Lett. B **341**, (1994) 238.

[6] VENUS Collab., S. Uehara et al., Z. Phys. C **63**, (1994) 213.

[7] AMY Collab., T. Aso et al., Phys. Lett. B **363**, (1995) 249, Phys. Lett. B **381**, (1996) 372.

[8] ALEPH Collab., D. Buskulic et al., Phys. Lett. B **355**, (1995) 595.

[9] L3 Collab., M. Acciarri *et al.*, Phys. Lett. B **453**, (1999) 83.

[10] L3 Collab., B. Adeva *et al.*, Nucl. Inst. Meth. **A 289** (1990) 35;
M. Acciarri *et al.*, Nucl. Inst. Meth. **A 351** (1994) 300;
M. Chemarin *et al.*, Nucl. Inst. Meth. **A 349** (1994) 345;
I.C. Brock *et al.*, Nucl. Inst. Meth. **A 381** (1996) 236;
A. Adam *et al.*, Nucl. Inst. Meth. **A 383** (1996) 342.

[11] J.A.M. Vermaseren, Nucl. Phys. B **229**, (1983) 347.

[12] T. Sjöstrand, Comput. Phys. Commun. **82**, (1994) 74.

[13] S. Jadach, B.F.L. Ward and Z. Was, Comput. Phys. Commun. **79**, (1994) 503.

[14] M. Skrzypek, S. Jadach, W. Placzek and Z. Was, Comput. Phys. Commun. **94**, (1996) 216.

[15] M. Cacciari et al., Nucl. Phys. B **466**, (1996) 173.

[16] G.A. Schuler and T. Sjöstrand, Z. Phys. C **68**, (1995) 607; Phys. Lett. B **376**, (1996) 193.

[17] V. M. Budnev et al., Phys. Rep. **15** (1975) 181.

[18] The L3 detector simulation is based on GEANT Version 3.14; see R. Brun et al., GEANT 3, CERN DD/EE/84-1 (Revised), September 1987 and the GHEISHA program (H. Fesefeld, RWTH Aachen Report PITHA85/02 (1985)) for the simulation of hadronic interactions.

[19] The LEP Experiments: ALEPH, DELPHI, L3 and OPAL, Nucl. Inst. Meth. **A 378** (1996) 101.

[20] M. Cacciari et al., in CERN 96-01 Physics at LEP2, edited by G. Altarelli, (1996), v.1, p. 334.

[21] M. Glück, E. Reya and A. Vogt, Phys. Rev. D **46**, (1992) 1973.

[22] M. Drees and K. Grassie, Z. Phys. C **28**, (1985) 451.

[23] S. Nussinov, Phys. Rev. Lett. **35**, (1975) 1672;
G.J. Feldman et al., Phys. Rev. Lett. **38**, (1977) 1313.

[24] The LEP/SLD Heavy Flavour Working Group, Electroweak Heavy Flavour Results presented at the 1999 Winter Conferences, LEPHF/99-01, L3 Note 2392, 19 May 1999.

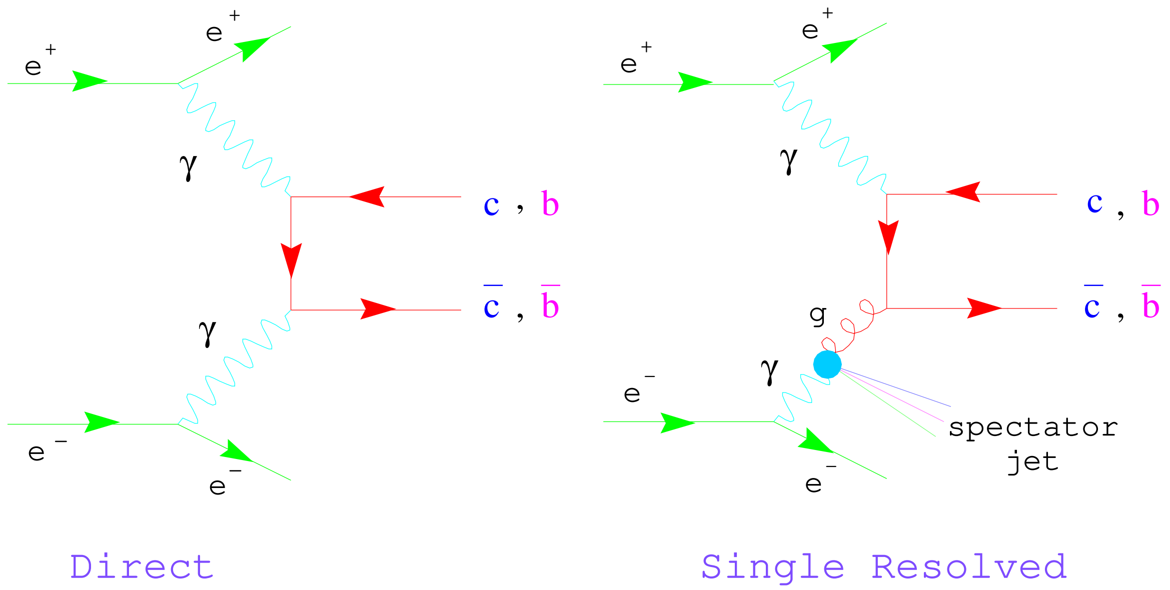

Figure 1: Diagrams contributing to charm production in $\gamma\gamma$ collisions at LEP. Contributions from other processes, double resolved process and VDM, are predicted to be small at LEP energies [1].

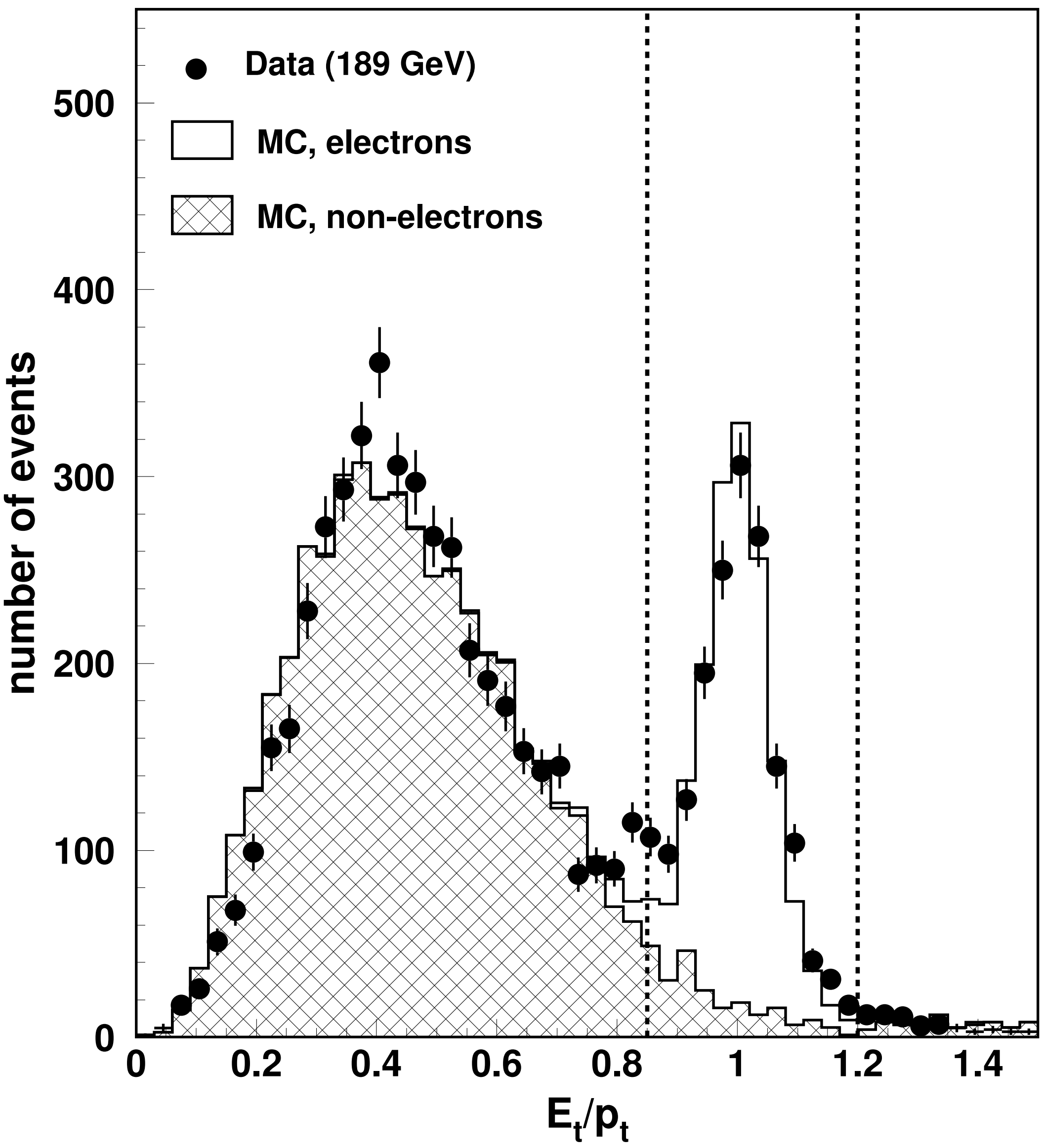

Figure 2: The ratio, E_t/p_t, of the transverse energy measured by the electromagnetic calorimeter and the transverse momentum of the track. A clear electron signal is observed at the expected value of $E_t/p_t = 1$. The window, defined by the dashed lines, of $0.85 < E_t/p_t < 1.2$ indicates the selected electron candidates.

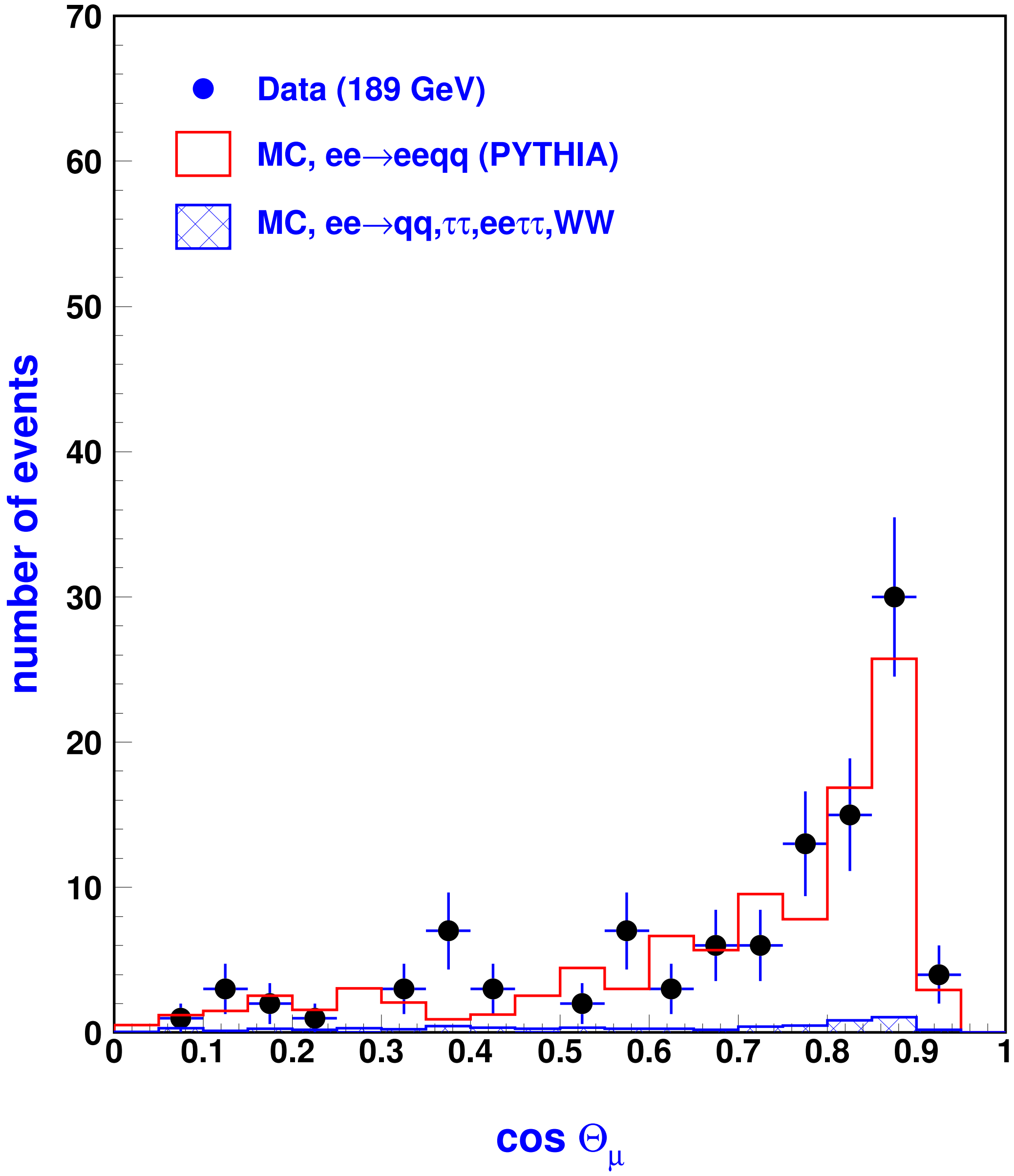

Figure 3: The polar angle distribution of the selected muon candidates.

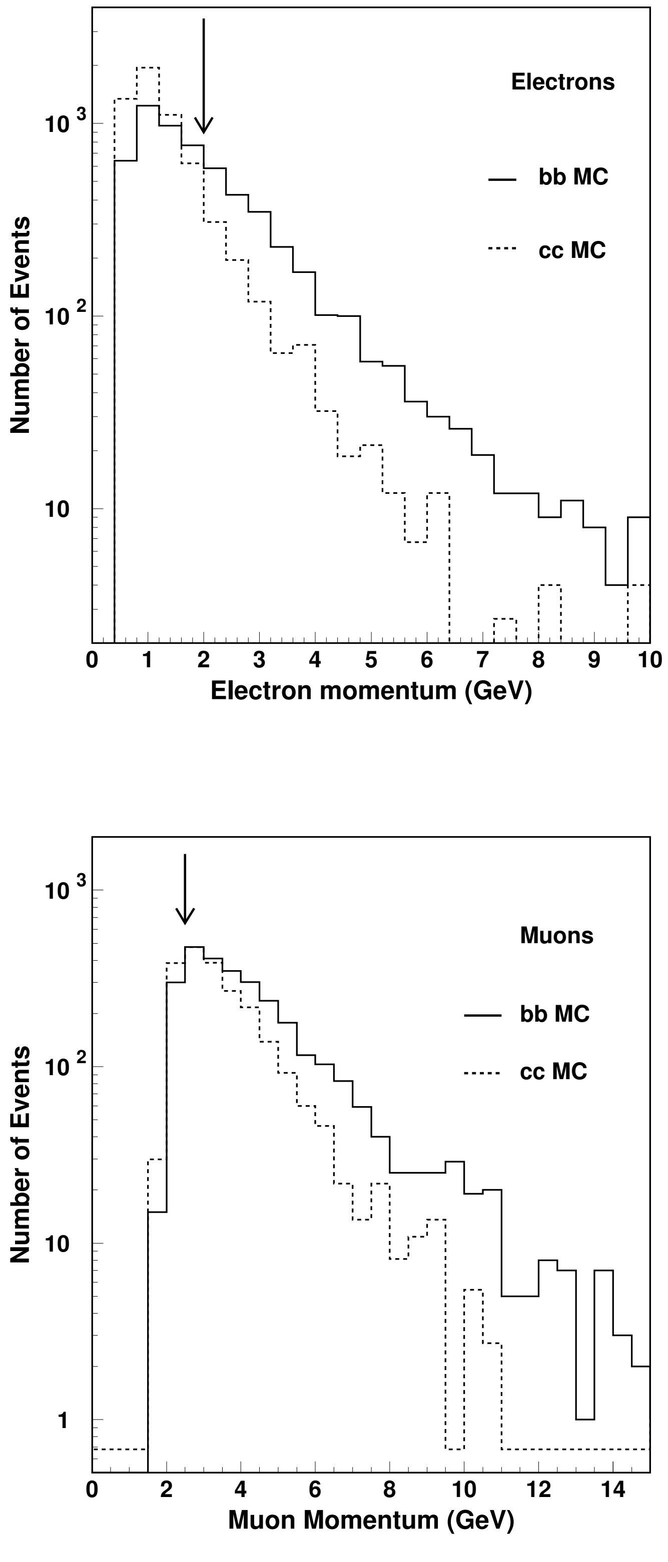

Figure 4: Electron and muon momentum in semi-leptonic b and c decays, as expected by JAMVG Monte Carlo generator.

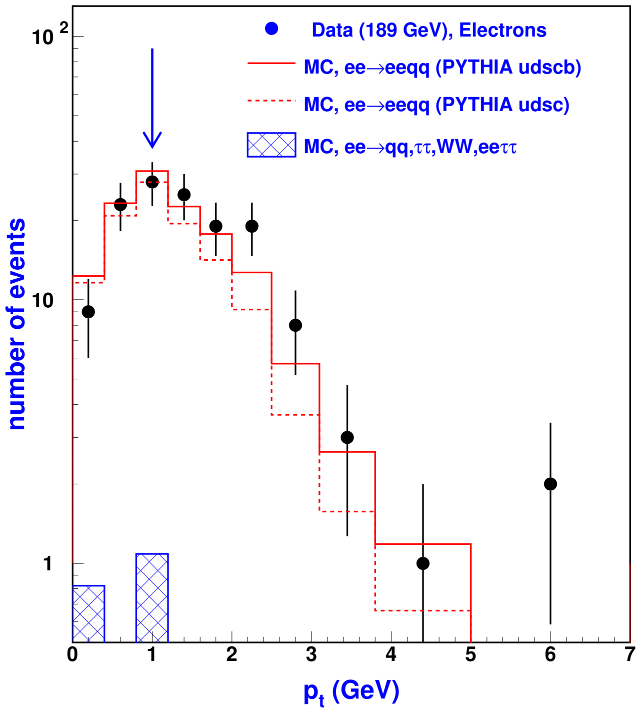

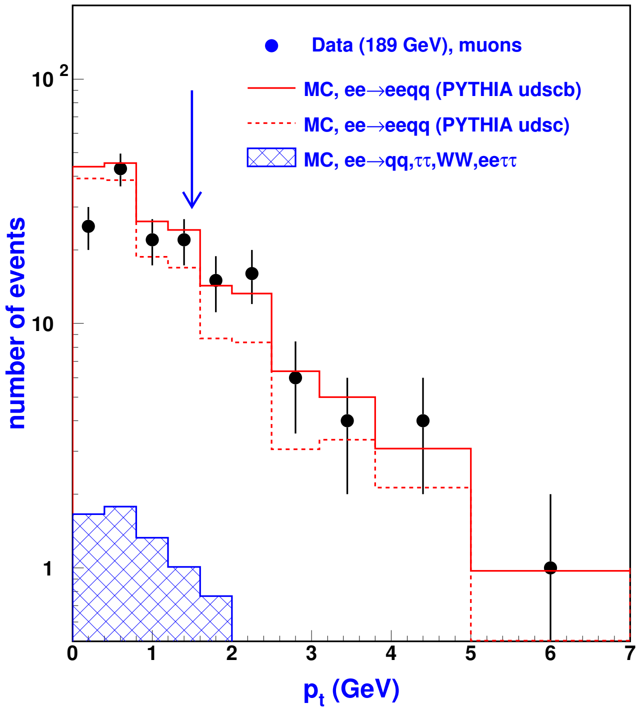

Figure 5: Electron and muon transverse momentum, p_t, with respect to the closest jet after the cut on the lepton momentum has been applied: $P_e > 2$ GeV and $P_\mu > 2.5$ GeV.

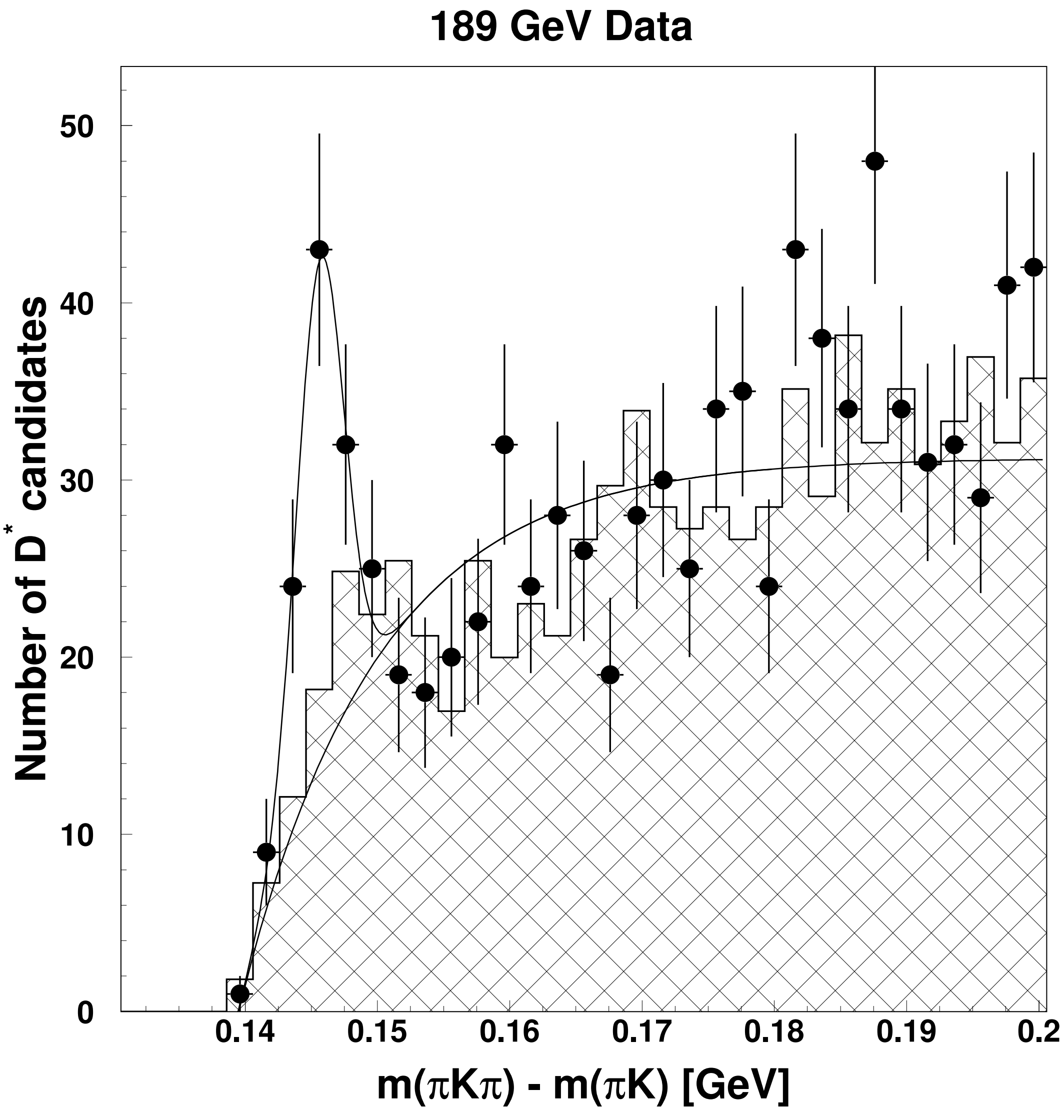

Figure 6: Mass difference $M_{D^*} - M_{D^0}$ for the $D^{*+} \to D^0\pi^+ \to K^-\pi^+\pi^+$ decay mode. The D^* signal is well identified as the peak at about 145 MeV. The shaded histogram shows the D^0 side-band and D^0 wrong-charge combination, which represents well the combinatorial background to the D^* signal.

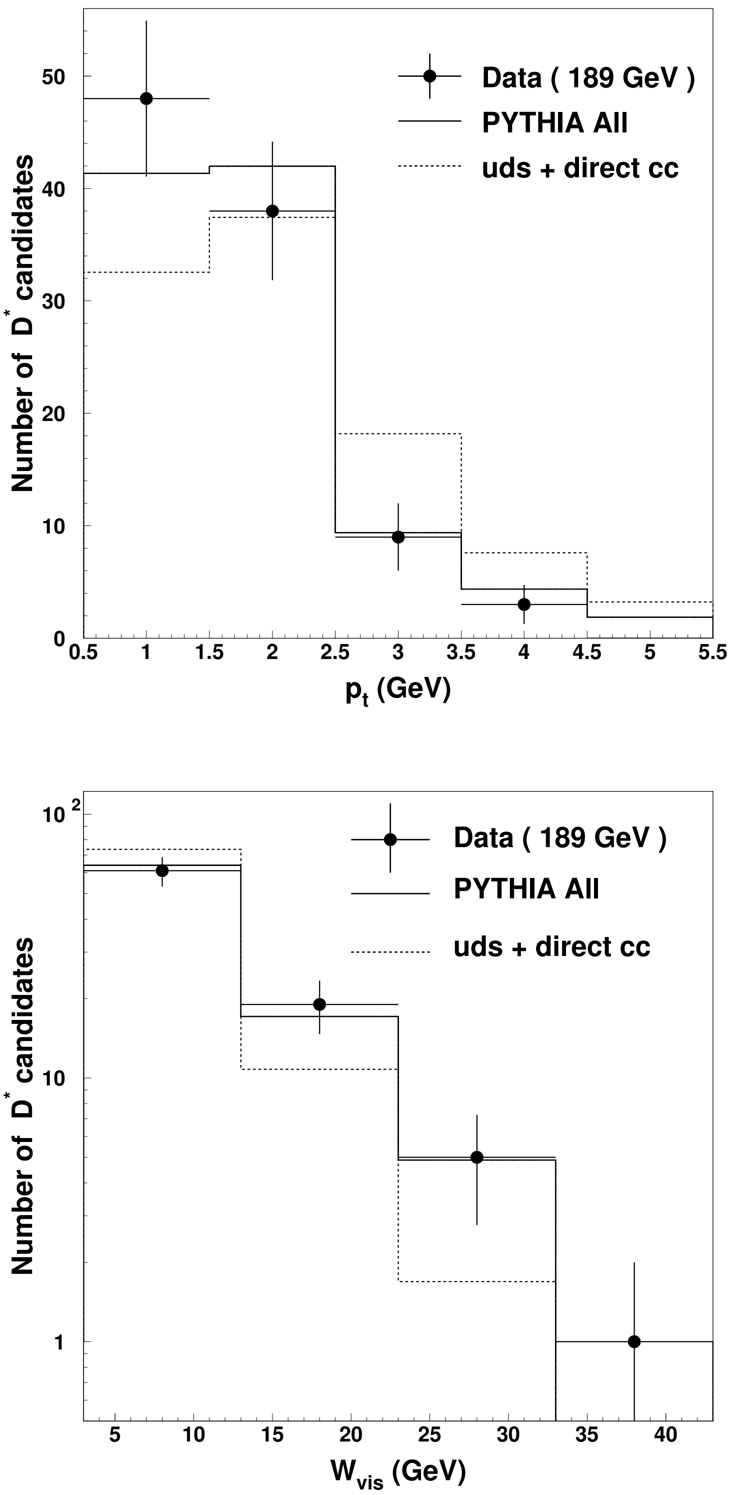

Figure 7: The D^* candidate transverse momentum and the event visible mass distributions are compared with PYTHIA prediction for the direct process only (dashed histogram) and for all processes included (solid histogram). In both cases the Monte Carlo is normalized to the number of data events.

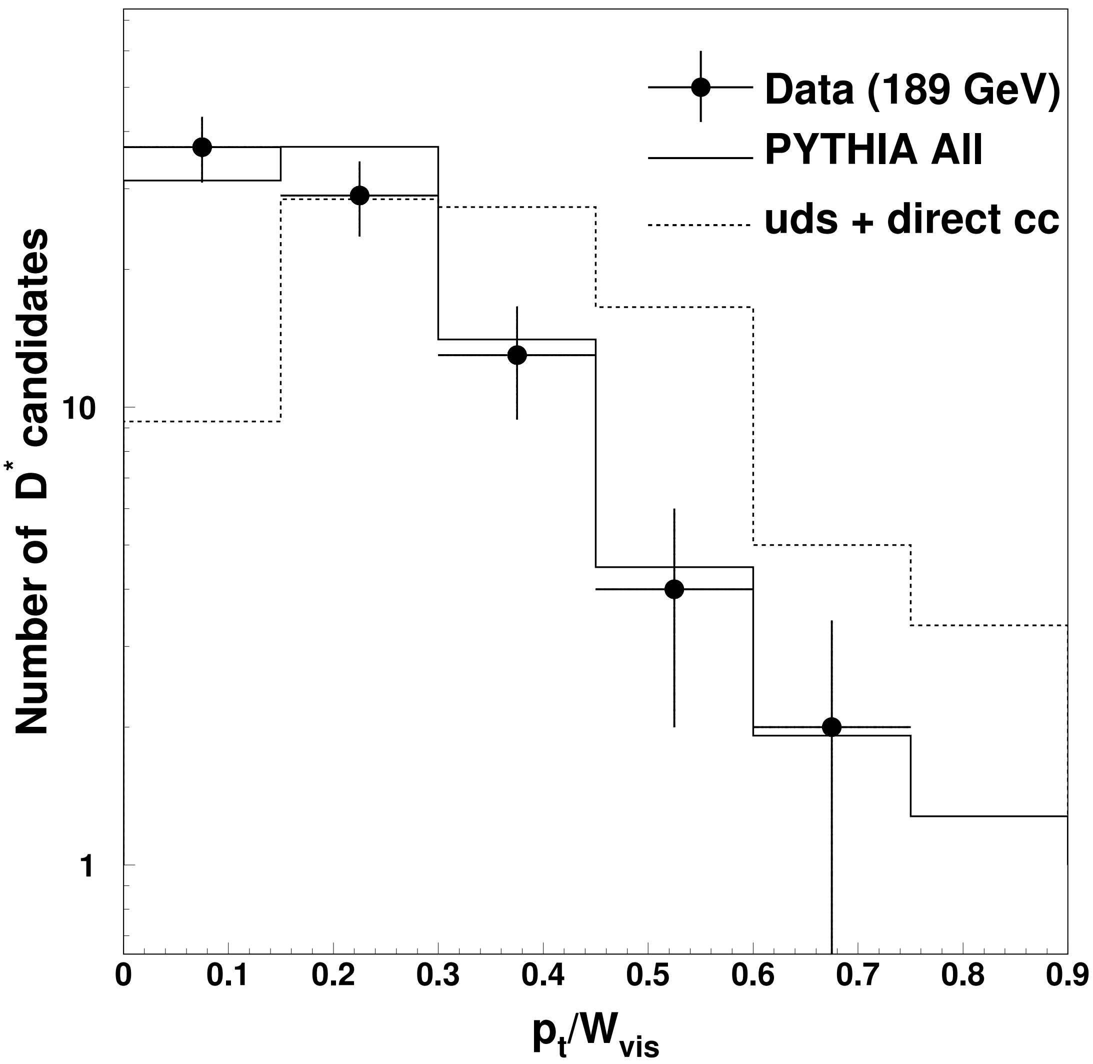

Figure 8: The data versus Monte Carlo comparison for the ratio $p_t^{D^*}/W_{vis}$. The PYTHIA prediction is shown for the direct process only (dashed histogram) and for all processes included (solid histogram). In both cases the Monte Carlo is normalized to the number of data events. The direct process alone can not describe the data, while the full PYTHIA model reproduces the data correctly.

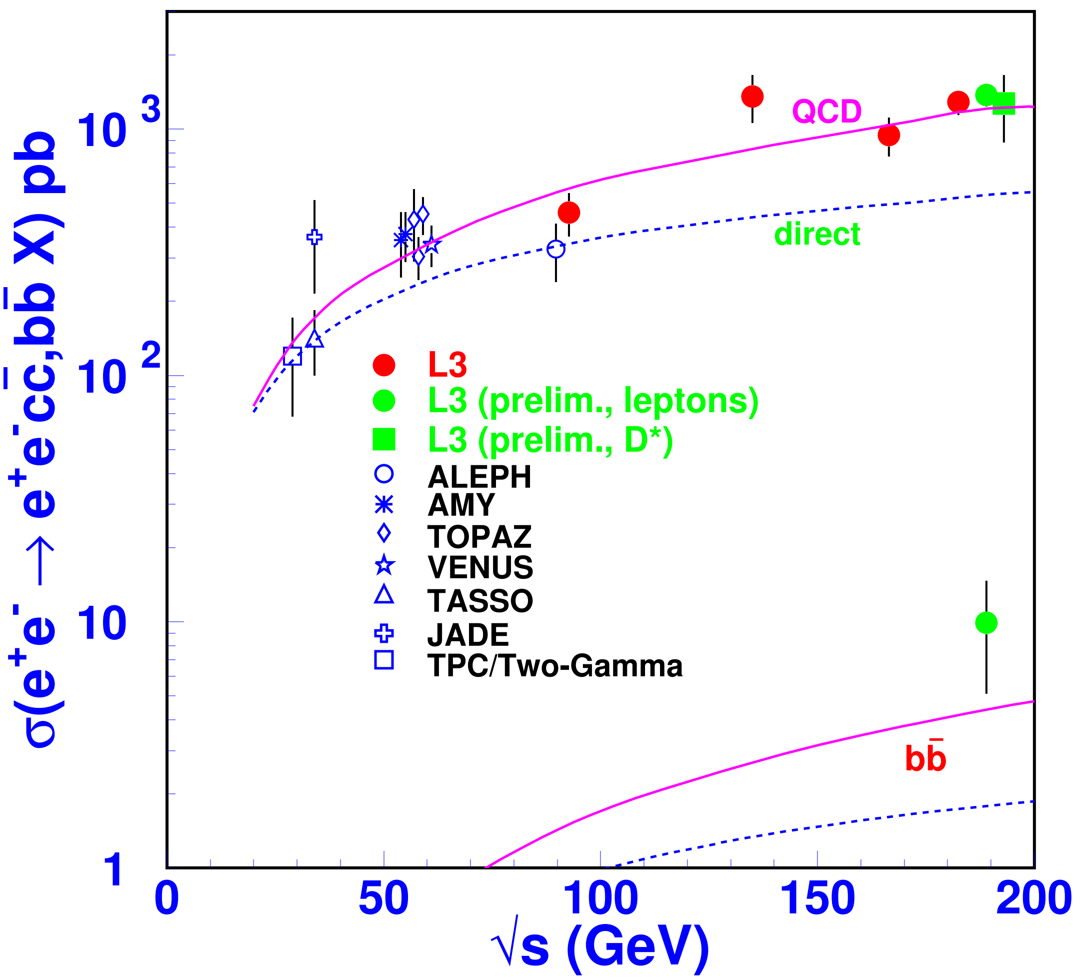

Figure 9: The charm and beauty production cross section in two-photon collisions. The L3 data from both the electron and the muon events are combined. The statistical and systematic errors are added in quadrature. The dashed line corresponds to the direct process prediction while the solid line shows the QCD prediction for the sum of the direct and the resolved processes calculated to NLO accuracy [1]. The prediction corresponds to a charm quark mass of 1.3 GeV, the parton density function of Glück-Reya-Vogt [21] and the renormalization scale chosen to be the charm quark mass. Points at $\sqrt{s} = 58$ GeV, $\sqrt{s} = 91$ GeV and $\sqrt{s} = 189$ GeV energies are artificially separated for clear visibility.